

Supplementary Information for:

A Remarkably Flexible and Selective Receptor for Ba²⁺ Amplified from a Hydrazone Dynamic Combinatorial Library

Jörg Klein,^{†a} Vittorio Saggiomo,^{†b} Lisa Reck,^b Mary McPartlin,^a G. Dan Pantos,^a Ulrich Lüning^{*b} and Jeremy K. M. Sanders^{*a}

^aUniversity Chemical Laboratory, University of Cambridge, Lensfield Road,
Cambridge CB2 1EW, United Kingdom
Fax: (+)44 (0)1223 336017
Email: jkms@cam.ac.uk

^b Otto-Diels-Institut für Organische Chemie, Olshausenstr. 40,
D-24098 Kiel, Germany.
Fax: +49-431-880-1558;
Tel: +49-431-880-2450
E-mail: luening@oc.uni-kiel.de

Synthesis	2
Library Preparation	3
LC-MS Analysis	3
Reversibility	4
Isolation of Macrocycles and Characterisation	4
UV-Vis Titrations	6
Crystallographic Data	9

General remarks

Solvents were purchased from Romil (LC-MS grade CHCl₃), Fischer (HPLC grade MeOH) and Aldrich (TFA). Metal salts were purchased from Sigma-Aldrich (RbCl), Lancaster (LiCl), Breckland (NaCl, KCl), Alpha Aesar (CsCl). 4-Methoxypyridine-2,6-dicarbaldehyde was synthesized according to literature.¹

¹H and ¹³C NMR spectra were recorded on Bruker DPX-400, DRX 500 or AV 600 or Advance 500 TCI Cryo Spectrometers. All signals were internal referenced to solvent residue (3.31 ppm for MeOD). All high-resolution (HR) electrospray ionisation (ESI) mass spectra were recorded on Waters LCT Premier XE instrument.

UV-Vis spectra were recorded in a 1cm quartz cuvette using a Lambda 14 spectrometer from Perkin Elmer at 22 °C, unless otherwise stated. The DCLs were analysed by LCMS using an Agilent 1100 series HPLC coupled to an Agilent XCT Ion-Trap.

¹ U. Lüning, R. Baumstark, K. Peters and H. G. von Schnering, Liebig's Ann. Chem., 1990, 129.

Synthesis

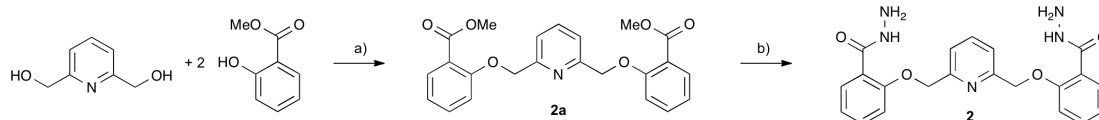


Fig. 1 Synthesis of 2. a) $\text{PPh}_3/\text{DIAD}/\text{THF}$, 34%; b) N_2H_4 , 90%.

2,6-Bis(2-carboxyphenoxy)methylpyridine (2a)

2,6-Di(hydroxymethyl)pyridine (500 mg, 3.60 mmol), salicylic acid methyl ester (1.37 mL, 10.8 mmol) and triphenylphosphine (2.36 g, 9.00 mmol) were dissolved in dry tetrahydrofuran (25 mL) and cooled to 0 °C. Under nitrogen, diisopropyl azodicarboxylate (2.1 mL, 10.8 mmol) was slowly added and the solution was afterwards stirred at room temperature for 48 h. The reaction mixture was hydrolysed with sodium hydroxide solution (2 N, 20 mL). After stirring for 15 minutes the layers were separated and the water layer was extracted with diethyl ether (2 x 15 mL). The combined organic layers were washed with water and brine and were dried over magnesium sulfate. The solvent was evaporated in vacuo and the residue was purified by column chromatography (silica gel, 0.04–0.063 mm, cyclohexane/ethyl acetate, 2:1 → 1:2) $R_f = 0.33$ in cyclohexane/ethyl acetate 2:1. After the chromatography the product was recrystallized from ethanol to yield a white solid (500 mg, 1.23 mmol, 34 %); **m.p.** 119 °C (Lit.^[2]: 120 °C). **$^1\text{H-NMR}$ (500 MHz, CDCl_3):** $\delta = 7.87$ (dd, $^3J = 7.7$ Hz, $^4J = 1.7$ Hz, 2 H, 6- $\text{C}_{\text{Ar}}\text{H}$), 7.84 (t, $^3J = 7.8$ Hz, 1 H, 4- $\text{C}_{\text{Py}}\text{H}$), 7.73 (d, $^3J = 7.8$ Hz, 2 H, 3,5- $\text{C}_{\text{Py}}\text{H}$), 7.46 (ddd, $^3J = 8.4$ Hz, $^3J = 7.4$ Hz, $^4J = 1.7$ Hz, 2 H, 4- $\text{C}_{\text{Ar}}\text{H}$), 7.04 – 6.98 (m, 4 H, 3,5- $\text{C}_{\text{Ar}}\text{H}$), 5.30 (s, 4 H, OCH_2), 3.94 (s, 6 H, OCH_3) ppm. **$^{13}\text{C-NMR}$ (125 MHz, CDCl_3):** $\delta = 166.5$ (COOCH_3), 157.8 (2- C_{Ar}), 156.3 (2,6- C_{Ar}), 138.1 (4- C_{Py}), 133.7 (4- C_{Ar}), 131.9 (6- C_{Ar}), 120.7 (5- C_{Ar}), 120.3 (1- C_{Ar}), 120.0 (3,5- C_{Py}), 113.4 (3- C_{Ar}), 70.8 (OCH_2), 52.0 (OCH_3) ppm. **IR (ATR):** $\tilde{\nu} = 3000$ (arom. C-H), 2940 (OCH_3), 1712 (C=O), 1233 (C-O-C), 1081 (Ar-O-C), 743 (1,2-disubst. benzene) cm^{-1} . **MS (ESI, positive mode, MeOH):** m/z (%): 430 (100) $[\text{M}+\text{Na}]^+$ 408 (10) $[\text{M}+\text{H}]^+$. **$\text{C}_{23}\text{H}_{21}\text{NO}_6$ (407.14):** calcd. C 67.80, H 5.20, N 3.44; found C 68.33, H 5.03, N 3.44.

2,6-Di(2-hydrazidophenoxy)methylpyridine (2)

2,6-Bis(2-methoxycarbonylphenoxy)methylpyridine (420 mg, 1.03 mmol) was added to a hydrazine hydrate solution (64 %, 20 mL). The solution was stirred at 110 °C for 2 h. After cooling down to room temperature the precipitated solid was filtered off and washed with ethanol. The product was recrystallized from ethanol yielding a white solid (380 mg, 0.93 mmol, 90 %); **m.p.** 201.5 °C. **$^1\text{H-NMR}$ (500 MHz, DMSO-d_6):** $\delta = 9.89$ (s, 2 H, NH), 7.92 (t, $^3J = 7.75$ Hz, 1H, 4- $\text{C}_{\text{Py}}\text{H}$), 7.76 (dd, $^3J = 7.5$ Hz, $^4J = 1.8$ Hz, 2 H, 6- $\text{C}_{\text{Ar}}\text{H}$), 7.51 (d, $^3J = 7.75$ Hz, 2 H, 3,5- $\text{C}_{\text{Ar}}\text{H}$), 7.45 (ddd, $^3J = 8.3$ Hz, $^3J = 7.5$ Hz, $^4J = 1.8$ Hz, 2 H, 4- $\text{C}_{\text{Ar}}\text{H}$), 7.20 (dd, $^3J = 8.3$ Hz, $^4J = 0.7$ Hz, 2 H, 3- $\text{C}_{\text{Ar}}\text{H}$), 7.07 (td, $^3J = 7.5$ Hz, $^4J = 0.7$ Hz, 2 H, 5- $\text{C}_{\text{Ar}}\text{H}$), 5.46 (s, 4 H, OCH_2), 4.62 (s, 4 H, NH_2) ppm. **$^{13}\text{C-NMR}$ (150 MHz, DMSO-d_6):** $\delta = 164.7$ (COON_2H_3), 156.0 (2- C_{Ar}), 155.6 (2,6- C_{Py}), 138.2 (4- C_{Py}), 132.0 (4- C_{Ar}), 130.3 (6- C_{Ar}), 122.8 (1- C_{Ar}), 121.1 (5- C_{Ar}), 120.5 (3,5- C_{Py}), 113.4 (3- C_{Ar}), 70.3 (CH_2) ppm. **IR (ATR):** $\tilde{\nu} = 3227$ (hydrazide), 1612 (C=O), 1052 (Ar-O-C), 749 (1,2-disubst. benzene) cm^{-1} . **MS (ESI):**

² L. L. Gumanov, A. A. Shteinman, E. Nordlander, G. I. Koldobskii, *Russ. J. Org. Chem.* **2002**, 38, 606–608.

m/z (%) = 430 (100) $[M+Na]^+$, $C_{21}H_{21}N_5O_4$ (**407.16**): calcd. C 61.91, H 5.20, N 17.19; found C 61.91, H 5.15, N 16.94.

Library Preparation

Templated DCLs were prepared by mixing stock solutions of building blocks (20 mM in $CHCl_3$) and metal salts (50 mM in MeOH) and adding the appropriate amount of $CHCl_3$ and MeOH. Exchange was initiated by addition of 5% TFA to the DCLs. DCLs were typically prepared on a 1 mL scale (1 mM, analytical for metal screening) or on a 10 mL scale (10 mM, preparative to isolate the 2+2 macrocycles).

LC-MS Analysis

After 14 days DCLs were analysed by LCMS using an Agilent 1100 series HPLC coupled to an Agilent XCT Ion-Trap. Water was obtained from a MilliQ purification system. MeOH (Fischer Scientific, LC-MS grade) and formic acid (Fluka, p.a. puriss. for mass spectrometry) were purchased from commercial suppliers. Samples were analysed using a Phenomenex Prodigy 5 ODS-2 column (150 x 4.60 mm, particle size: 5 μ m), an injection volume of 5 μ l, a flow rate of 1.0 ml/min and a gradient of MeOH in water (60 % to 70 % in 10 min, then to 100 % in 1 min, both containing 0.1 % formic acid) at 323 K. UV absorption was detected at 290 nm and referenced against 550 nm. Positive ion mass spectra were acquired in standard enhanced mode using electrospray ionisation (drying temperature: 350 °C; nebuliser pressure: 18 psi; drying gas flow: 8 l/min; ICC target: 200 000; range: 400-1700 m/z)

Reversibility

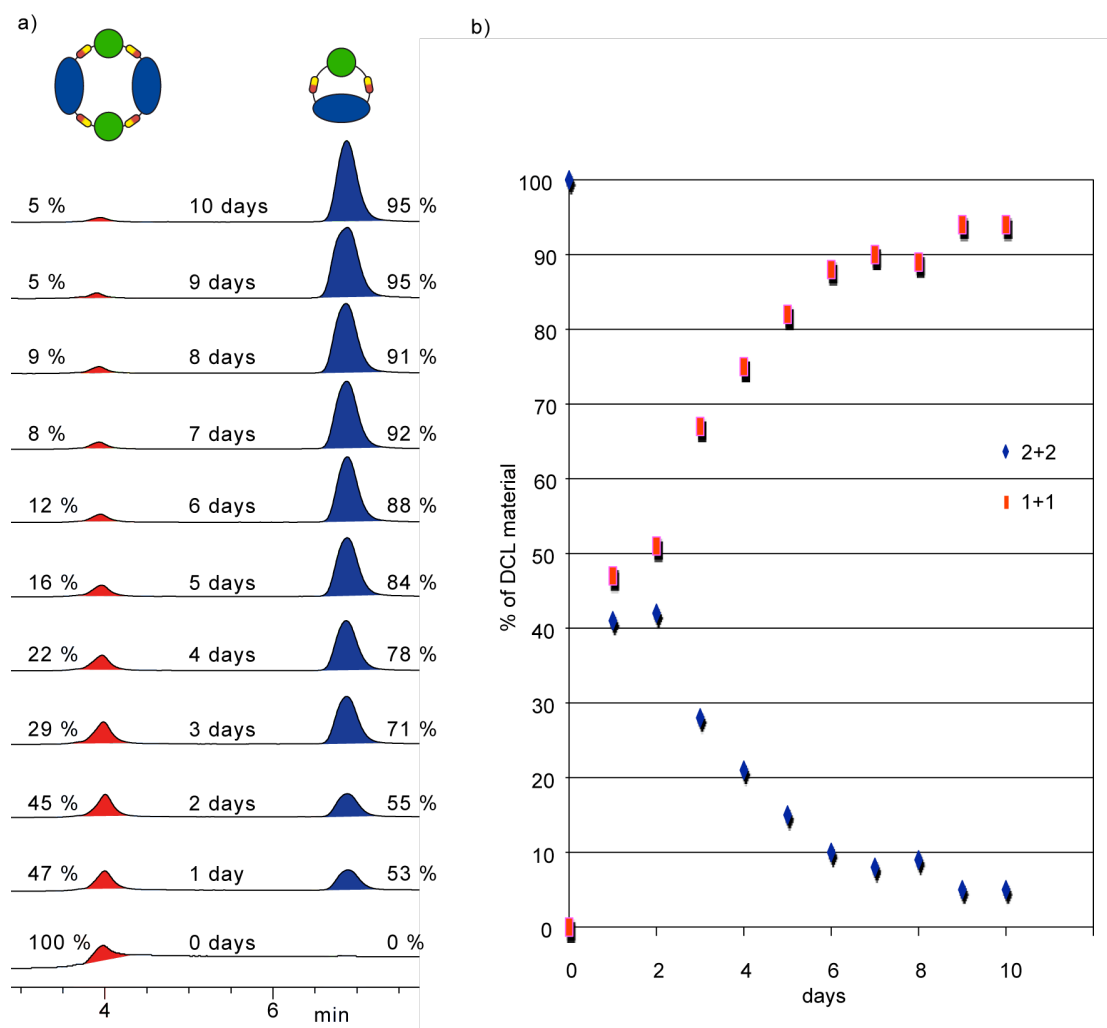


Fig. 2 Conversion of **4** into **3** over time.

The isolated sample of **4** was dissolved in $\text{CHCl}_3/\text{MeOH}/\text{TFA}$ (50/50/5, 1 mM) and stirred. Every day a sample of the mixture was taken, basified (to halt the exchange) and stored at -20°C . After 19 days the samples were analysed by LC MS and the relative peak of the two products (**3** and **4**) were plotted over time. Original DCL distribution was reached after approx. 10 days.

Isolation of Macrocycle and Characterisation

The 2+2 macrocycle, **4**, was isolated from a DCL at 10 mM in $\text{CHCl}_3/\text{MeOH}/\text{TFA}$ (90/10/5). After 10 days the precipitate was collected by filtration, washed with NaCO_3 (sat.) and dried *in vacuo*. The macrocycle was obtained as a white powder in 95 % yield. Complexes with metals were prepared by adding a solution of metal chloride (50 mM in MeOD) to a solution of the macrocycle ($\text{CDCl}_3/\text{MeOD}$, 1:1, CDCl_3 was filtered through alumina before use).

4

^1H NMR (400 MHz, 298 K, $\text{CDCl}_3/\text{MeOD}$, 1/1, v/v). δppm = 3.94 (s, 6H), 5.48 (s, 8H), 7.02 (d, 4H, $^3J = 8.4$ Hz), 7.08 (t, 4H, $^3J = 7.5$ Hz), 7.39 (t, 4H, $^3J = 7.6$ Hz), 7.60 (s, 4H), 7.67 (d, 4H, $^3J = 7.5$ Hz), 7.90 (m, 6H), 8.03 (s, 4H).

^{13}C -NMR (125 MHz, 300 K, $\text{CDCl}_3/\text{MeOD}$, 1/1, v/v). δppm = 56.9, 72.5, 109.5, 114.4, 122.4, 123.1, 123.7, 132.8, 134.9, 149.2, 155.5, 157.3, 157.6, 162.9, 163.2, 165.2.

HRMS (ESI+) calcd. for $\text{C}_{58}\text{H}_{48}\text{N}_{12}\text{O}_{10}$: $[\text{MH}]^+$ (m/z) = 1073.3689, found: 1073.3909; $[\text{MH}_2]^{2+}/2$ (m/z): 537.1881, found: 537.1949.

4·Ba

^1H NMR (400 MHz, 298 K, $\text{CDCl}_3/\text{MeOD}$, 1/1, v/v). δppm = 4.01 (s, 6H), 5.41 (s, 8H), 6.91 (t, 4H, $^3J = 7.5$ Hz), 7.08 (d, 4H, $^3J = 8.4$ Hz), 7.20 (s, 4H), 7.33 (t, 4H, $^3J = 8.0$ Hz), 7.46 (dd, 4H, $^3J = 7.7$ Hz, $^5J = 1.3$ Hz), 7.50 (d, 4H, $^3J = 7.8$ Hz), 7.88 (t, 2H, $^3J = 7.8$ Hz), 8.31 (s, 4H).

^{13}C -NMR (125 MHz, 300 K, $\text{CDCl}_3/\text{MeOD}$, 1/1, v/v). δppm = 57.3, 71.4, 114.4, 115.0, 121.8, 122.8, 123.8, 132.2, 135.2, 139.9, 148.2, 155.6, 157.2, 158.0, 167.2, 169.9.

HRMS (ESI+) calcd. for $\text{C}_{58}\text{H}_{46}\text{N}_{12}\text{O}_{10}\text{Ba}$: $[\text{MH}]^+$ (m/z) = 1209.2585, found: 1209.2639; $[\text{MH}_2]^{2+}/2$ (m/z): 605.2010, found: 605.1326.

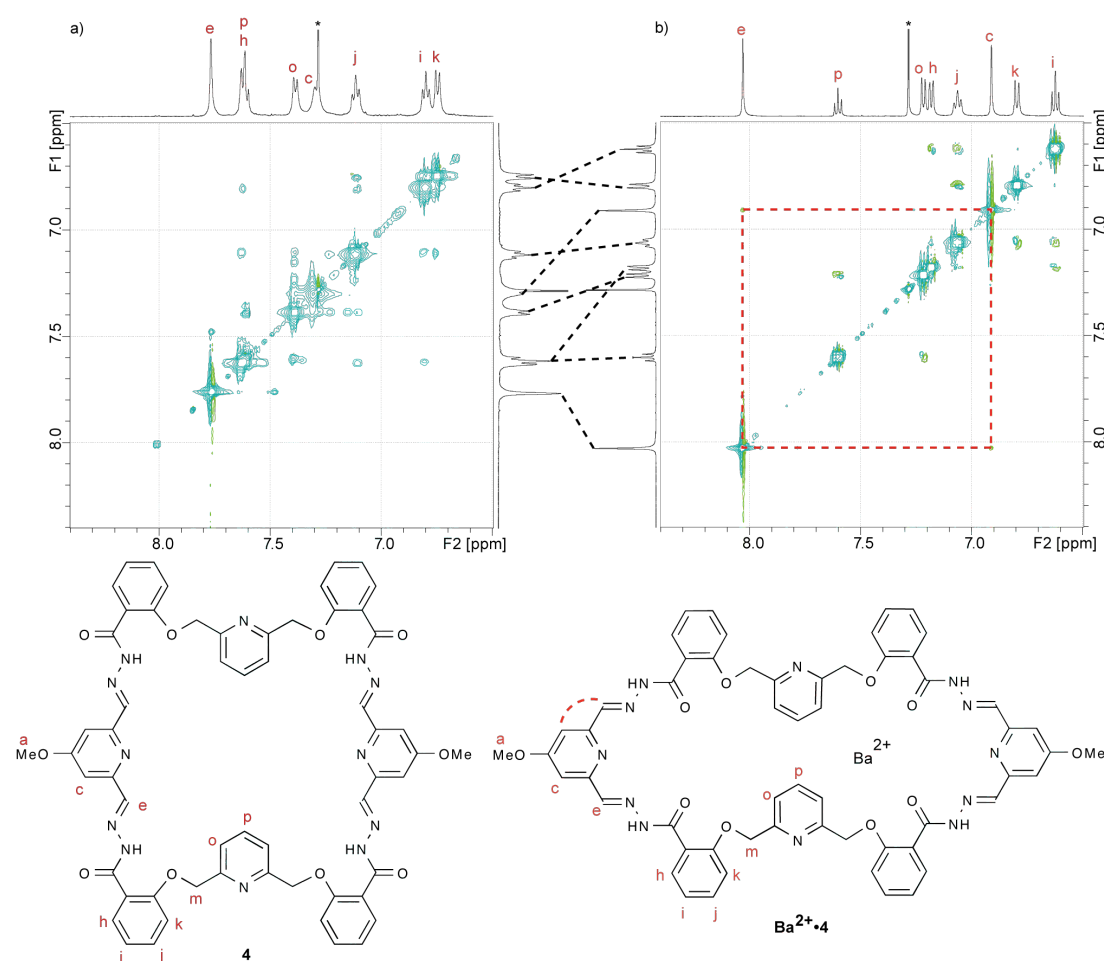


Fig. 3 Partial NOESY spectra (500 MHz, $\text{CDCl}_3/\text{MeOD}$ (1/1), K, $d_8 = 800$ ms) of a) **4** and b) its Ba^{2+} complex **4·Ba**. The appearance of the indicated cross-peak (red, dotted

line) suggests a conformational change upon binding. Corresponding peaks are connected by dotted lines. Residual solvent peaks are marked with an asterisk.

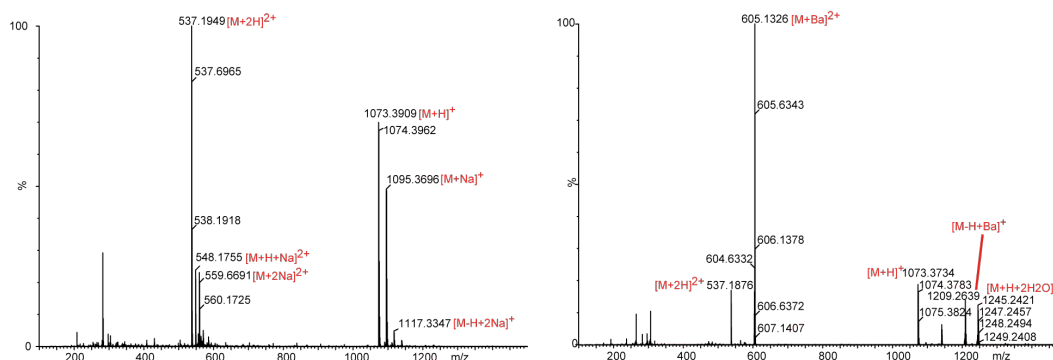


Fig. 4 HRMS (+ESI) spectra of **4** (left) and **4·Ba** (right).

UV-Vis Titrations

Host **4** was dissolved in CHCl₃/MeOH (1/1,v/v) to solutions of 0.02 mM. Metal salts were dissolved to solutions of 50 mM in MeOH.

Procedure of the binding studies involved making sequential additions of metal salts using Eppendorf pipettes to a 2.500 ml solution of **4** in a spectrometric cell ($b = 1$ cm). UV-Vis spectra were then combined to produce plots that showed the changes in the spectral features as a function of changes in the concentration of metal salts.

Binding constant was calculated using a model derived by Maarten Smolders³. The resulting equation, of the form,

$$y = Y0 + DY \left(\frac{(K_a(P+x)+1) - \sqrt{((K_a(P+x)+1)^2 - 4K_a^2Px)}}{(2K_aP)} \right)$$

was computer fit using the Origin version 7 software package, where

x = total guest concentration [MCl_2],

y = change in absorption dA,

$Y0$ = absorption of **4** at 273 nm,

P = total host concentration ($[\textbf{4}] = 0.02$ mM),

DY = absorption of **4·Ba** at 273,

K_a = binding constant.

The change in absorbance, ΔA , was calculated at a $\lambda = 273$ nm where the spectral change was maximal.

³ Y. R. Hristova, M. M. J. Smulders, J. K. Clegg, B. Breiner and J. R. Nitschke, *Chem. Sci.*, DOI:10.1039/C0SC00495B.

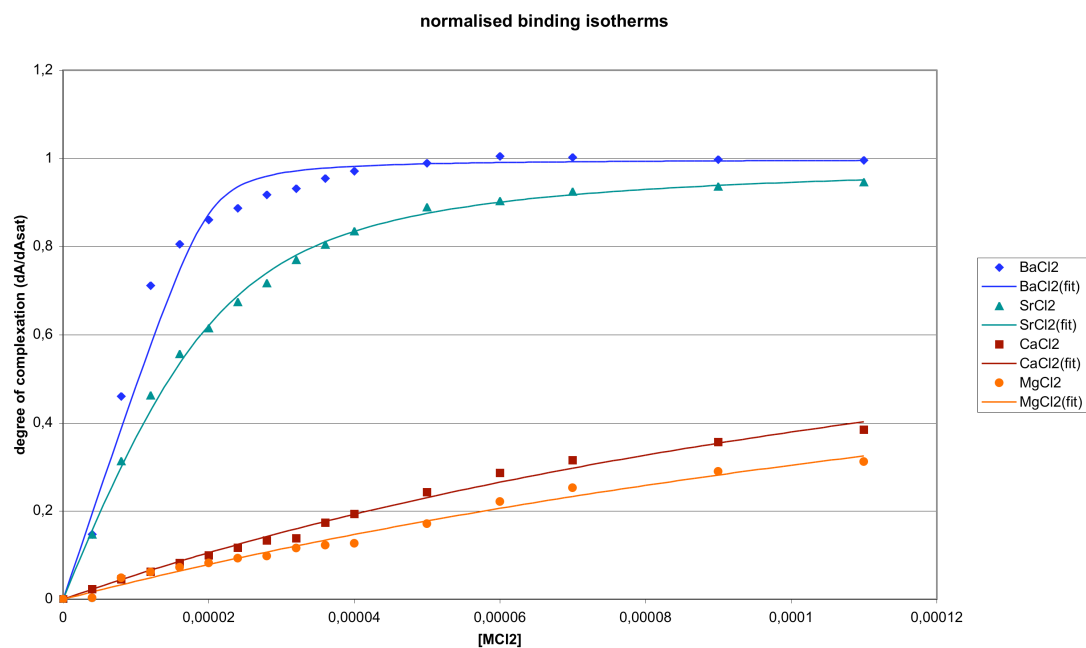


Fig. 5 Binding isotherms for the binding of different guests to **4** at 23 °C. The binding strength increases in the order $\text{MgCl}_2 < \text{CaCl}_2 < \text{SrCl}_2 < \text{BaCl}_2$.

Table 1 Binding constants for **4** with different metal salts.

guest	K_a	error
MgCl_2 (23 °C)	4660	1387
CaCl_2 (23 °C)	6622	1237
SrCl_2 (23 °C)	217337	18057
BaCl_2 (23 °C)	$>10^6$	n/a
BaCl_2 (33 °C)	500960	111332
BaCl_2 (43 °C)	339600	62078

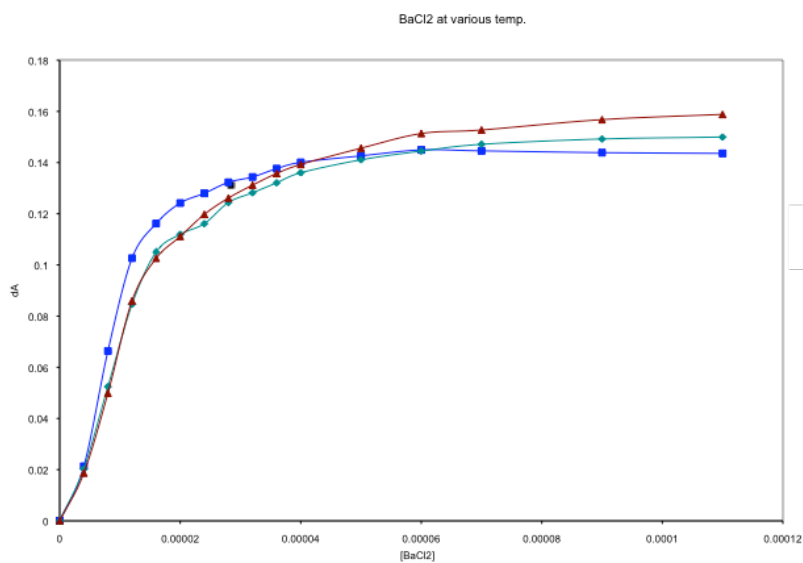


Fig. 6 Binding isotherms of the binding of BaCl_2 to **4** at different temperatures. At higher temperature the binding becomes weaker and more reliable data was obtained.

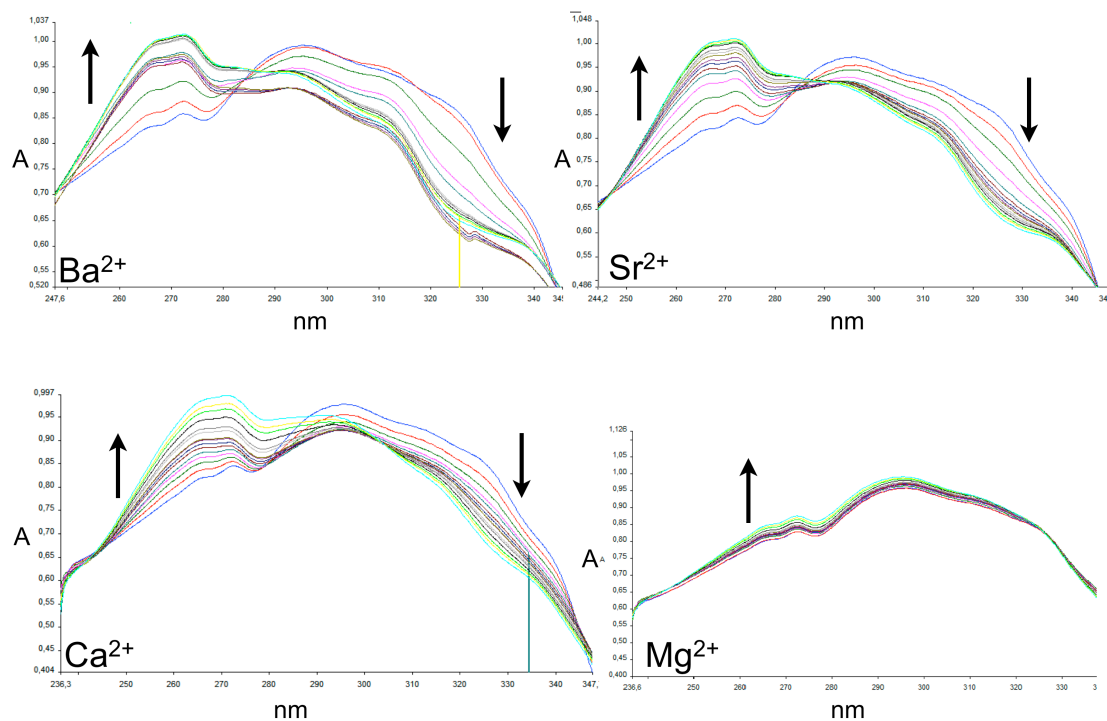


Fig. 7 Spectra of the UV titrations.

Crystallographic Data

Data for $4 \cdot 1.5\text{H}_2\text{O} \cdot 4\text{CHCl}_3$ were collected on a Nonius Kappa FR590 diffractometer employing graphite-monochromated Mo-K α radiation generated from a sealed tube (0.71073 Å) with ω and ψ scans at 180(2) K.⁴ Data integration and reduction were undertaken with HKL Denzo and Scalepack.⁵ Subsequent computations were carried out using the WinGX-32 graphical user interface.⁶ The structure was solved by direct methods using SIR92.⁷ Multi-scan empirical absorption corrections, when applied, were applied to the data set using the program SORTAV.⁸ Data were refined and extended with SHELXL-97.⁹ In general, non-hydrogen atoms with occupancies of greater than 0.5 were refined anisotropically, Carbon-bound and nitrogen-bound hydrogen atoms were included in idealised positions and refined using a riding model. The water hydrogen atoms could not be located in the difference Fourier map and were not included. Considerable disorder of the chloroform solvates was indicated by high ADPs and additionally one pyridyl group of the macrocycle was resolved into two components of ca 60:40 % occupancy. There are two CHCl_3 molecules with 40:60 occupancies in the vicinity of this disorder. There is a total of 1.5 H_2O solvates in the asymmetric unit. One H_2O is near the centre of the macrocycle ring and the second half molecule is disordered across an inversion centre. A number of restraints and constraints were required to facilitate realistic modelling of the disorder. The extensive solvate disorder explains the poor diffraction at high angle resulting in a low data to parameter ratios and relatively high R values.

Table 2 Hydrogen Bond Geometry

Donor	Hydrogen	Acceptor	D-H(Å)	H-A(Å)	D-A(Å)	DHA Angle(°)
N(3B)	H(3B)	O(3B)	0.86	2.08	2.667(5)	124.9
N(3B)	H(3B)	N(1')	0.86	2.10	2.720(15)	128.8
N(3B)	H(3B)	N(1)	0.86	2.20	2.796(10)	126.1
N(3A)	H(3A)	O(1W)	0.86	2.11	2.931(5)	160.0
N(5A)	H(5A)	O(4A)	0.86	2.09	2.671(6)	124.4
N(5A)	H(5A)	N(2B) ⁱ	0.86	2.50	2.945(6)	112.6
N(5B)	H(5B)	O(4B)	0.86	2.16	2.698(5)	120.2
N(5B)	H(5B)	N(4B)	0.86	2.40	3.204(5)	155.5

Symmetry Operator

ⁱ $-x+1, -y+1, -z$

4 Nonius. BV, COLLECT, Nonius BV, Delft, The Netherlands, 1998

5 Z. Otwinowski and W. Minor, Methods in Enzymology, 1997, 276, 307-326.

6 L. Farrugia, J. Appl. Cryst., 1999, 32, 837-838.

7 A. Altomare, M. C. Burla, M. Camalli, G. Cascarano, C. Giacovazzo, A. Guagliardi and G. Polidori, J. Appl. Cryst., 1994, 27, 435.

8 R. H. Blessing, Acta Cryst., 1995, A51, 33-38.

9 G. M. Sheldrick, SHELXL-97: Programs for Crystal Structure Analysis, University of Göttingen, Germany, 1997.

Discussion

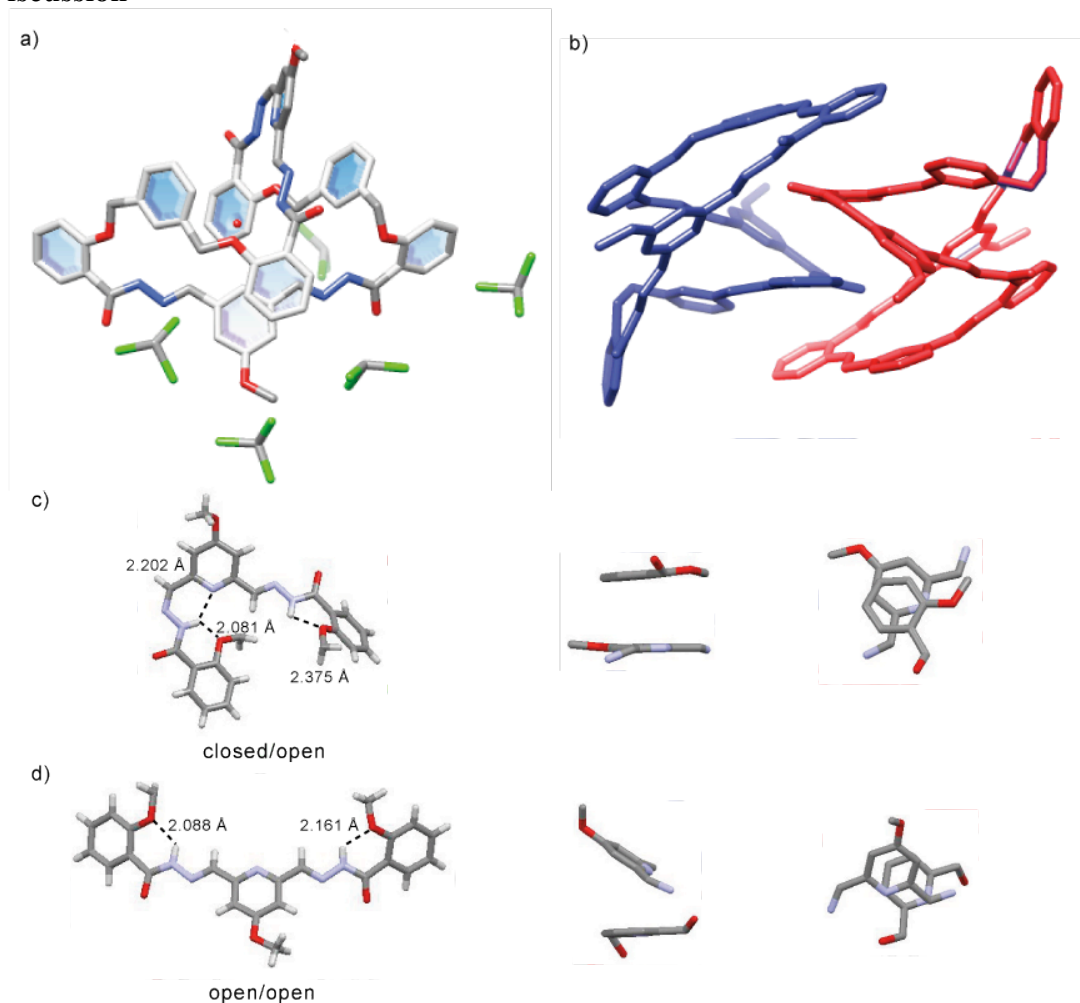


Fig. 8 Schematic representation of the crystal structure of $4 \cdot 1.5\text{H}_2\text{O} \cdot 4\text{CHCl}_3$. Hydrogen bonds are indicated by black dotted lines. a) molecular structure with solvent molecules; b) dimer of intercalated enantiomers; c) asymmetrically oriented hydrazones and π -stacks found in the top end of the molecule in a); d) symmetrically oriented hydrazones and π -stacks found in the lower end of the molecule in a).

$4 \cdot 1.5\text{H}_2\text{O} \cdot 4\text{CHCl}_3$ crystallises in the triclinic space group $P\bar{1}$ with one molecule in the asymmetric unit. A solvent water molecule is located within the macrocycle, forming a number of hydrogen bonds with the hydrazone moieties. **4** is highly twisted becoming helical (Fig. 8a). Each of the twisted macrocycles represents an enantiomer (Fig. 8b). As the space group contains inversion symmetry a racemic mixture of the two *P* and *M* enantiomers is present throughout the lattice. The manner in which the molecules twist can be effectively described using “open/closed” nomenclature (Fig. 8c-d). π - π Stacking interactions and several hydrogen bonds (Fig. 8c-d) stabilize the folding of the macrocycle. Adjacent pairs of enantiomers are partially intercalate and linked together through hydrogen bonding interactions between the macrocycles and their guest water molecules (space group, Fig. 8**Error! Reference source not found**.b).